scientific reports

OPEN

Room-temperature bonding of Al_2O_3 thin films deposited using atomic layer deposition

Ryo Takakura, Seigo Murakami, Kaname Watanabe & Ryo Takigawa

In this study, room-temperature wafer bonding of Al_2O_3 thin films on Si thermal oxide wafers, which were deposited using atomic layer deposition (ALD), was realized using the surface-activated bonding (SAB) method. Transmission electron microscopy (TEM) observations indicated that these room-temperature-bonded Al_2O_3 thin films appeared to work well as nanoadhesives that formed strong bond between thermally oxidized Si films. The perfect dicing of the bonded wafer into dimensions of 0.5 mm × 0.5 mm was successful, and the surface energy, which is indicative of the bond strength, was estimated to be approximately 1.5 J/m^2. These results indicate that strong bonds can be formed, which may be sufficient for device applications. In addition, the applicability of different Al_2O_3 microstructures in the SAB method was investigated, and the effectiveness of applying ALD Al_2O_3 was experimentally verified. This successful SAB of Al_2O_3 thin films, which is a promising insulator material, opens the possibility of future room-temperature heterogenous integration and wafer-level packaging.

Room-temperature bonding technology has emerged as a challenging process for three-dimensional integration and wafer-level packaging of optoelectronics, MEMS, RF, and CMOS devices. As a technique for direct bonding, hydrophilic bonding via plasma activation is becoming mainstream in the semiconductor industry[1–3]. This method requires annealing at a temperature of a few hundred degrees to achieve a sufficiently strong bond for practical applications. To overcome the severe thermal stress and degradation of bond alignment accuracy, the development of room-temperature bonding technology is essential.

As one solution, surface-activated bonding (SAB)[4] is a promising room-temperature direct bonding technology. In this method, wafer surfaces are first irradiated using an argon (Ar) fast atom beam (FAB) to remove organic contaminants and the native oxide layer, and then, the activated wafer surfaces are brought into contact at room temperature. The applicability of this method to various materials has been studied for a wide range of device applications. To date, the SAB method has demonstrated room-temperature bonding of metals (Cu–Cu[5,6] and Au–Au[7,8]) as well as semiconductors (Si–Si[9], Ge–Ge[10], Si–GaAs[11], Si–SiC[12], and GaAs–SiC[13]). However, it is difficult to apply this method to the direct bonding of SiO_2 and SiN, which are suitable as insulator layer materials in semiconductor device applications[14,15]. To overcome this limitation, modified SAB[16–19] and atomic diffusion bonding[20,21] have been reported based on the quasi-direct bonding concept using a metal intermediate layer. In addition, a room-temperature bonding method using an Si intermediate layer has recently been reported[22–25]. In some electronics applications such as 3D integration using vertical electrical interconnections, these intermediate layers cause serious current leakage. Therefore, the SAB of insulating materials is highly desirable.

Al_2O_3 is a promising alternative insulator material because of its excellent electrical resistivity and thermal conductivity, which are comparable to those of SiO_2. To date, the SAB of single-crystal Al_2O_3[26], SAB of Al_2O_3 deposited by mist CVD[27], and hydrophilic bonding of Al_2O_3[28], which requires annealing at 100–300 °C after temporary bonding, have recently been examined. Herein, we focus on Al_2O_3 thin films grown by atomic layer deposition (ALD), which allows for precise growth, atomic-scale thickness control, and good uniformity on large-scale wafers. Previous reports on Al_2O_3 thin films deposited by ALD, have investigated hydrophilic bonding[29,30] and modified SAB[31], in which an adhesive of Si is sputter-deposited on ALD-deposited Al_2O_3 films. SAB[32] of AlO films deposited by ion beam sputtering has also been examined. It is interesting to apply ALD Al_2O_3 thin films to the SAB method.

There have only been a few studies on the application of the SAB method to the direct bonding of ALD Al_2O_3 thin films without a heating process, and a large bond strength has not yet been achieved. Herein, the

Graduate School of Information Science and Electrical Engineering, Kyushu University, 744 Motooka, Nishi-ku, Fukuoka 819-0395, Japan. email: takigawa@ed.kyushu-u.ac.jp

applicability of the SAB method to the direct bonding of ALD Al_2O_3 thin films is investigated in comparison with those of single-crystal sapphire. Furthermore, we demonstrate the room-temperature wafer direct bonding of deposited Al_2O_3 thin films on a Si thermal oxide wafer using the ALD method. Compared to previous reports, the novelty of this study is the utilization of a surface-activated bonding method using Ar-FAB for Al_2O_3 thin films deposited by ALD.

Results and discussion

SAB of ALD Al_2O_3 thin films on 4-inch Si thermal oxide wafers was performed at room temperature. Ar FAB irradiation was used for surface activation. Surface smoothness is one of critical factors for room-temperature direct bonding, and a rms of approximately 0.5 nm or less is typically required[33]. First, the wafer surfaces were studied before and after Ar FAB irradiation using atomic force microscopy (AFM). Figure 1 shows an AFM image of the ALD Al_2O_3 surface over a measured area of 1 μm × 1 μm. Consequently, the RMS surface roughness of the ALD Al_2O_3 thin film was 0.32 nm and 0.25 nm before and after the Ar FAB irradiation, respectively. This indicates that Ar FAB irradiation for surface activation did not roughen the surface significantly, and the surface of the ALD Al_2O_3 film retained sufficient smoothness.

Figure 2 shows the infrared (IR) transmission image of the SiO_2–SiO_2 interface bonded with ALD Al_2O_3 thin films, showing no large voids in the entire bonded wafer. The bond strength was evaluated using the crack-opening method[34] and the half-cutting dicing test. In the crack-opening method, a razor blade is inserted into the bond interface, and the surface energy, which indicates the bond strength, can be calculated using the propagated crack length. Using the measured crack length, the estimated surface energy of ALD Al_2O_3–ALD Al_2O_3 was approximately 1.5 J/m^2. The dicing test of the bonded wafer was then performed using a dicing saw.

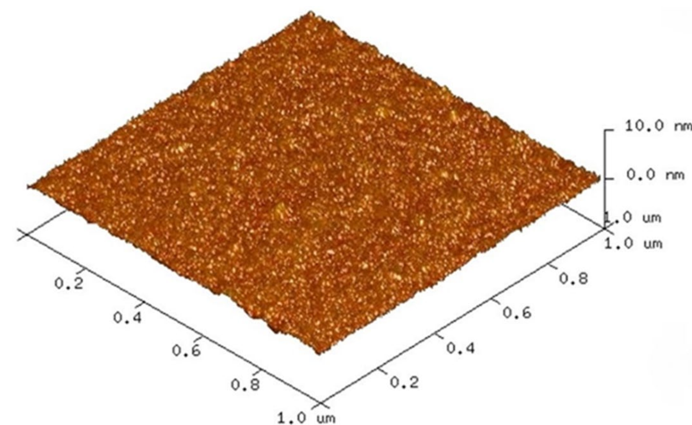

Figure 1. AFM image of the deposited Al_2O_3 thin film using ALD method.

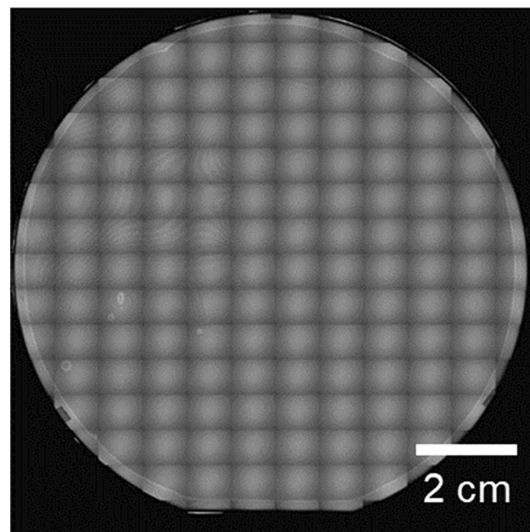

Figure 2. IR image of 4-inch-scale bonded thermal oxidized Si–Si wafer with ALD Al_2O_3 thin films at room temperature.

The bonded wafer was cut into 10-mm-square chips, and then one chip was half-cut into 0.5-mm-square pieces, leaving the bottom of the chip. The durability against the applied stress during the dicing process indicates the bond strength. As shown in Fig. 3, perfect dicing was successful with no debonding or chipping observed. These results indicate that a strong bond between ALD Al_2O_3 thin films can be achieved, which may be sufficient for device applications.

The nanostructure of the cross-sectional bonding interface was observed using transmission electron microscopy (TEM). Figure 4a,b show the TEM images obtained at low and high magnifications, respectively. The dotted line in Fig. 4b shows the initial bond interface of the ALD Al_2O_3 thin film.

As shown in Fig. 4b, a void-free bonding interface could be achieved at the atomic level, indicating the presence of a strong bond. In addition, we can see no damaged layer by Ar FAB irradiation, whereas this damaged layer clearly exists in the SAB of sapphire–sapphire.

These results indicate that the bonded ALD Al_2O_3 thin films functioned as adhesives and facilitated strong bond formation between two SiO_2 films. Figure 5 shows the results of elemental analysis obtained using energy-dispersive X-ray spectroscopy (EDX). Figure 5a shows a scanning TEM (STEM) image; the numbers in the image indicate EDX measurement points, and Fig. 5b shows the element concentrations at each measurement point. The elemental analysis of the bonded ALD Al_2O_3 in the depth direction (Fig. 5b) shows that there is little change in composition from the bonding interface in the depth direction (measurement points 4–6).

The bond strengths of the different Al_2O_3 were investigated. Figure 6 compares the bond strengths of sapphire–sapphire (SA–SA), sapphire–ALD Al_2O_3 (SA–ALD), and ALD Al_2O_3–ALD Al_2O_3 (ALD–ALD). Using the crack-opening method, the estimated surface energies of the bonded SA–SA, SA–ALD, and ALD–ALD were approximately 2.0, 1.9, and 1.5 J/m^2, respectively. It is well-known that the typical Al_2O_3 thin film deposited by ALD is amorphous. As shown in Fig. 4, no lattice structure was visible in the bonded ALD Al_2O_3 thin film, indicating that it was amorphous. As shown in Fig. 7, the measured X-ray diffraction (XRD) results also indicated that the Al_2O_3 thin film deposited by ALD is amorphous.

On the other hands, although sapphire has a single-crystalline structure, an amorphous-like layer (thickness ≈ 1 nm) exists at the bond interface owing to Ar FAB irradiation[27]. We can see that this crystal defect layer has little effect on the bonding strength because sufficient bond strength can be achieved compared with that of amorphous

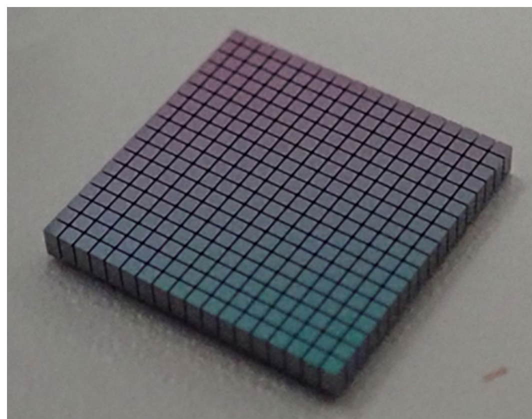

Figure 3. Image of the diced 0.5 mm × 0.5 mm chips, showing perfect dicing without debonding.

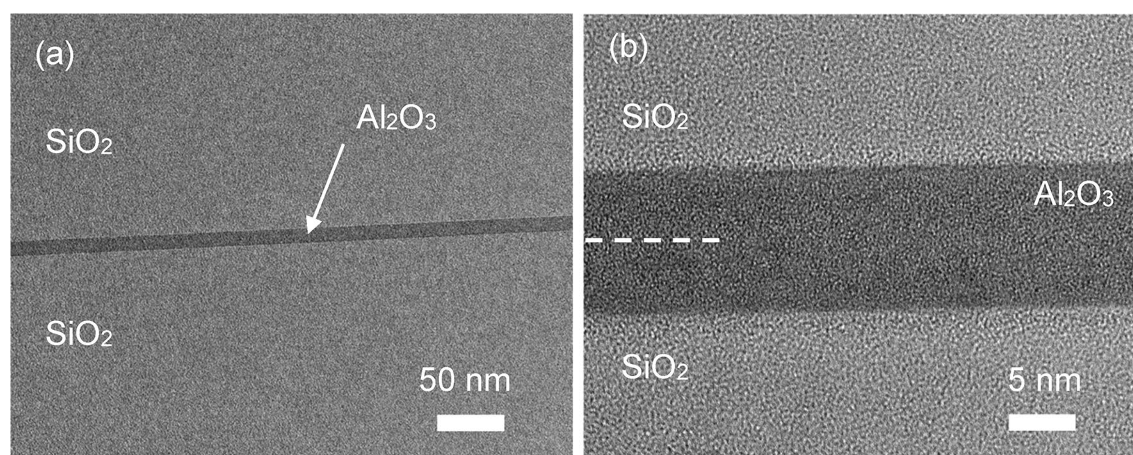

Figure 4. (**a**) Low- and (**b**) high-magnification cross-sectional TEM images of the bonding interface.

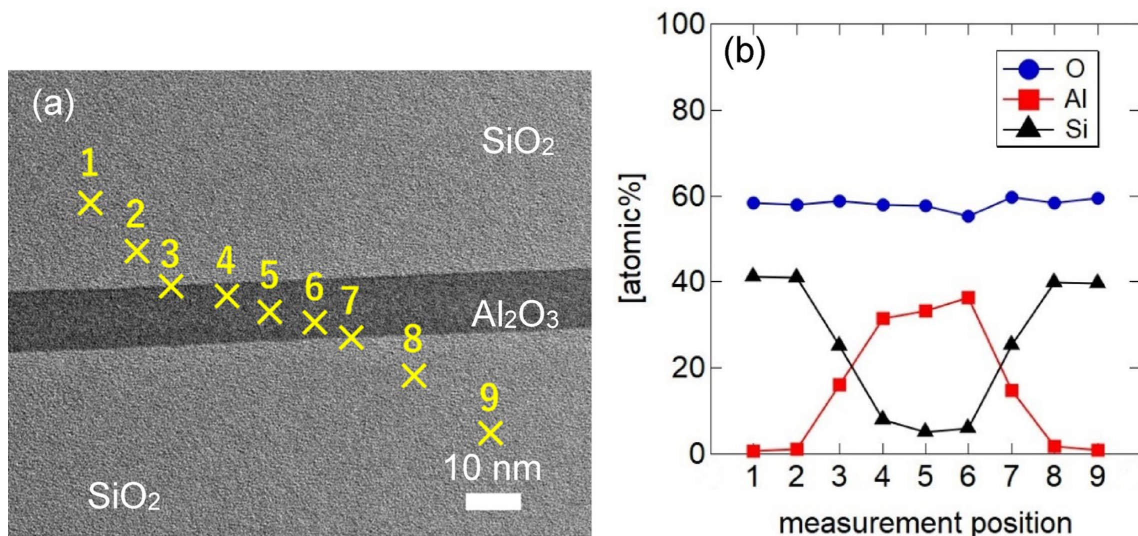

Figure 5. Elemental analysis using cross-sectional STEM-EDX.

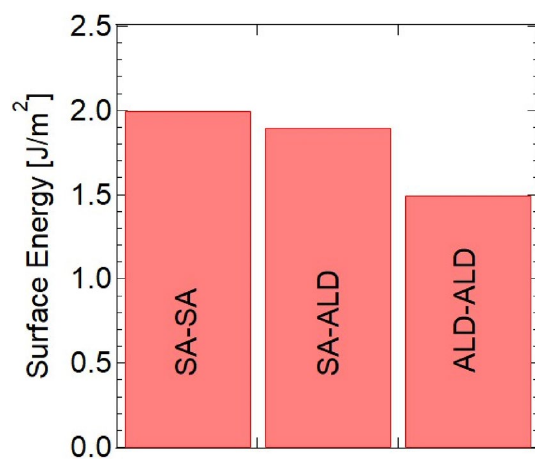

Figure 6. Comparison of the bond strengths of different Al_2O_3 samples.

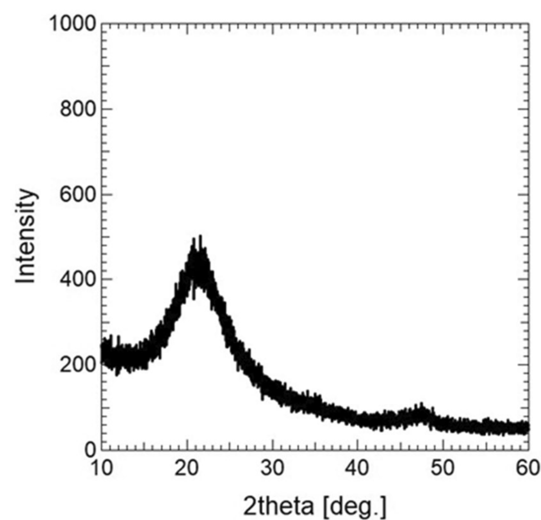

Figure 7. XRD pattern of ALD Al_2O_3 thin film.

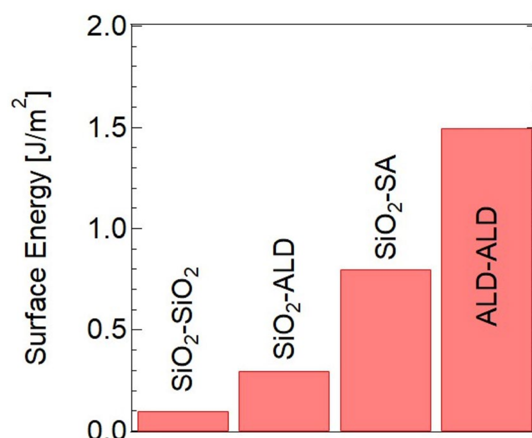

Figure 8. Comparison of bond strengths between SiO_2 and different Al_2O_3 samples.

Al_2O_3 thin films. We confirmed that the Al_2O_3 thin film-sapphire bond was weaker than the sapphire–sapphire bond. These results suggest that the crystallinity of the activated surface affects the bond strength of Al_2O_3. In addition, the experimental results demonstrated that the ALD method is suitable for the SAB of Al_2O_3 thin films.

Next, SAB of SiO_2–SiO_2, SiO_2–ALD Al_2O_3 (SiO_2–ALD), SiO_2–SA (SiO_2–sapphire), and ALD Al_2O_3–ALD Al_2O_3 (ALD–ALD) was performed under the same bonding conditions. Figure 8 shows a comparison of the bond strengths between SiO_2 and different Al_2O_3 samples. The low bond strengths of SiO_2–SiO_2 and SiO_2–ALD were confirmed, with the bond strength of SiO_2–ALD being slightly larger. Comparatively, the bond strength of SiO_2–SA was larger than both. This indicates that simply changing one of the wafers to one with better crystallinity tends to increase bond strength. However, it was necessary to form ALD Al_2O_3 films on both SiO_2 sides and bond them to achieve a sufficient strong SiO_2–SiO_2 bond interface for device applications. These results also suggest that the single-crystalline phase of Al_2O_3 is more effective, and crystallinity is important from the viewpoint of bond strength.

Conclusion

Herein, the SAB method was successfully applied to achieve the room-temperature wafer bonding of ALD Al_2O_3 thin films. The bonded ALD Al_2O_3 thin films appear to work well as nanoadhesives and form a strong bond between SiO_2 surfaces. The bonded wafer was perfectly diced into dimensions of 0.5 mm × 0.5 mm, and the surface energy, indicative of the bond strength, was estimated to be approximately 1.5 J/m^2. These results indicate that strong bonds that are sufficient for device applications can be achieved. In addition, the applicability of different Al_2O_3 microstructures to the SAB method was investigated, and the effectiveness of applying ALD Al_2O_3 was experimentally verified. This successful SAB of Al_2O_3 thin film, which is a promising insulator material, opens the possibility of future room-temperature heterogenous integration and wafer-level packaging. In additions, the results of this work will be of significant use in the development of fabrication technique for X materials-on-insulators using room temperature bonding method with ALD Al_2O_3 thin film, and not only SiO_2–SiO_2 bond interface.

Methods

In our experiments, we used an ultrathin Al_2O_3 film (thickness = 6 nm) deposited by atomic layer deposition (ALD) on a 4-inch wafer with a 1-μm thermal oxide film. The ALD deposition process used trimethylaluminum (TMA) as a precursor and ozone (O_3) as an oxidant. The deposition temperature was 400 °C. Post-deposition annealing was not performed.

Bonding was performed using a wafer-level bonding apparatus (MWB-08-AX, NIDEC MACHINE TOOL CORPORATION). For the bonding process, two wafer surfaces were simultaneously irradiated with Ar-FAB in a vacuum chamber at 5.1×10^{-6} Pa. The FAB irradiation conditions were as follows: voltage was 1.5 kV, current was 100 mA, Ar flow rate was 13 sccm, and FAB irradiation time was 30 s.. After FAB irradiation, the FAB-irradiated surfaces of the wafers were immediately brought into contact with each other in a vacuum apparatus, and a load of 9.8×10^4 N was applied for 10 s. for bonding.

X-ray diffraction (XRD) method was used to evaluate the crystallinity of ALD Al_2O_3 thin films. In-plane measurements were performed with an X-ray incidence angle of 0.5 degrees (the critical angle was 0.4 degrees).

The roughness of the deposited surface was evaluated using atomic force microscopy (AFM, DimensionIcon, Bruker). The nanostructure and elemental composition of the bonding interface were analyzed by TEM (Hitachi Hitech H9500) and STEM-EDX (Hitachi Hitech G4000).

Data availability

The datasets used and/or analyzed during the current study available from the corresponding author on reasonable request.

Received: 11 October 2022; Accepted: 21 February 2023
Published online: 03 March 2023

References

1. Pasquariello, D. & Hjort, K. Plasma-assisted InP-to-Si low temperature wafer bonding. *IEEE J. Sel. Top. Quant. Electron.* **8**, 118 (2002).
2. Suni, T., Henttinen, K., Suni, I. & Mäkinen, J. Effects of plasma activation on hydrophilic bonding of Si and SiO_2. *J. Electrochem. Soc.* **149**, G348 (2002).
3. Fujino, M., Takahashi, K., Ariga, Y. & Kikuchi, K. 300 mm wafer-level hybrid bonding for Cu/interlayer dielectric bonding in vacuum. *Jpn. J. Appl. Phys.* **59**, SBBA02 (2020).
4. Suga, T., Takahashi, Y., Takagi, H., Gibbesch, B. & Elssner, G. Structure of Al–Al and Al–Si_3N_4 interfaces bonded at room temperature by means of the surface activation method. *Acta Metall. Mater.* **40**(Supplement), S133 (1992).
5. Kim, T. H., Howlader, M. M. R., Itoh, T. & Suga, T. Room temperature Cu–Cu direct bonding using surface activated bonding method. *J. Vac. Sci. Technol. A* **21**, 449 (2003).
6. Shigetou, A. *et al.* Bumpless interconnect through ultrafine Cu electrodes by means of surface-activated bonding (SAB) method. *IEEE Trans. Adv. Packag.* **29**, 218 (2006).
7. Takigawa, R., Higurashi, E., Suga, T. & Sawada, R. Room-temperature bonding of vertical-cavity surface-emitting laser chips on Si substrates using Au microbumps in ambient air. *Appl. Phys. Exp.* **1**, 112201 (2008).
8. Matsumae, T., Kurashima, Y. & Takagi, H. Surface activated bonding of Ti/Au and Ti/Pt/Au films after vacuum annealing for MEMS packaging. *Microelectron. Eng.* **197**, 76 (2018).
9. Takagi, H., Kikuchi, K., Maeda, R., Chung, T. R. & Suga, T. Surface activated bonding of silicon wafers at room temperature. *Appl. Phys. Lett.* **68**, 2222 (1996).
10. Higurashi, E. *et al.* Room-temperature direct bonding of germanium wafers by surface-activated bonding method. *Jpn. J. Appl. Phys.* **54**, 030213 (2015).
11. Higurashi, E., Okumura, K., Nakasuji, K. & Suga, T. Surface activated bonding of GaAs and SiC wafers at room temperature for improved heat dissipation in high-power semiconductor lasers. *Jpn. J. Appl. Phys.* **54**, 030207 (2015).
12. Liang, J. *et al.* Electrical properties of p-Si/n-GaAs heterojunctions by using surface-activated bonding. *Appl. Phys. Express* **6**, 021801 (2013).
13. Liang, J., Nishida, S., Arai, M. & Shigekawa, N. Effects of thermal annealing process on the electrical properties of p+-Si/n-SiC heterojunctions. *Appl. Phys. Lett.* **104**, 161604 (2014).
14. Takagi, H., Maeda, R. & Suga, T. Wafer-scale spontaneous bonding of silicon wafers by argon-beam surface activation at room temperature. *Sens. Actuators A* **105**, 98 (2003).
15. Takagi, H., Utsumi, J., Takahashi, M. & Maeda, R. Room-temperature bonding of oxide wafers by Ar-beam surface activation. *ECS Trans.* **16**, 531 (2008).
16. Howlader, M. M. R., Okada, H., Kim, T. H., Itoh, T. & Suga, T. Wafer level surface activated bonding tool for MEMS packaging. *J. Electrochem. Soc.* **151**, G461 (2004).
17. Suga, T. *et al.* Silicon carbide wafer bonding by modified surface activated bonding method. *Jpn. J. Appl. Phys.* **54**, 030214 (2015).
18. Takigawa, R., Tomimatsu, T., Higurashi, E. & Asano, T. Residual stress in lithium niobate film layer of LNOI/Si hybrid wafer fabricated using low-temperature bonding method. *Micromachines* **10**, 136 (2019).
19. Takigawa, R. *et al.* Demonstration of GaN/$LiNbO_3$ hybrid wafer using room-temperature surface activated bonding. *ECS. J. Solid State Sci Technol.* **9**, 045005 (2020).
20. Shimatsu, T. & Uomoto, M. Atomic diffusion bonding of wafers with thin nanocrystalline metal films. *J. Vac. Sci. Technol. B* **28**, 706 (2010).
21. Ichikawa, M. *et al.* High-output-power deep ultraviolet light-emitting diode assembly using direct bonding. *Appl. Phys. Express* **9**, 072101 (2016).
22. Takigawa, R. & Asano, T. Thin-film lithium niobate-on-insulator waveguides fabricated on silicon wafer by room-temperature bonding method with silicon nanoadhesive layer. *Opt. Express* **26**, 24413 (2018).
23. Utsumi, J., Ide, K. & Ichiyanagi, Y. Cu/SiO_2 hybrid bonding obtained by surface-activated bonding method at room temperature using Si ultrathin films. *Micro Nano Eng.* **2**, 1 (2019).
24. Takigawa, R. *et al.* Fabrication of a bonded LNOI waveguide structure on Si substrate using ultra-precision cutting. *Jpn. J. Appl. Phys.* **59**, SBBD03 (2020).
25. Watanabe, K., Utsumi, J. & Takigawa, R. Bonding of $LiNbO_3$ and Si wafers at room temperature using Si nanolayers. *Jpn. J. Appl. Phys.* **60**, SCCL14 (2021).
26. Takagi, H., Kurashima, Y., Takamizawa, A., Ikegami, T. & Yanagimachi, S. Surface activated room-temperature bonding in Ar gas ambient for MEMS encapsulation. *Jpn. J. Appl. Phys.* **57**, 02BA04 (2018).
27. Utsumi, J. & Takigawa, R. Surface activated bonding of aluminum oxide films at room temperature. *Scr. Mater.* **191**, 215 (2021).
28. Chong, G. Y. & Tan, C. S. PE-TEOS wafer bonding enhancement at low temperature with a high-κ dielectric capping layer. *ECS Trans.* **28**, 489 (2010).
29. Li, Y. *et al.* Room temperature wafer bonding by surface activated ALD-Al_2O_3. *ECS Trans.* **50**, 303 (2013).
30. Beche, E. *et al.* Direct bonding mechanism of ALD-Al_2O_3 thin films. *ECS J. Solid State Sci. Technol.* **4**, P171 (2015).
31. Matsumae, T. *et al.* Room temperate bonding of Al_2O_3 layers by atomic layer deposition on polyimide substrates. *ECS Trans.* **69**, 99 (2015).
32. Takeuchi, K., Mu, F., Matsumoto, Y. & Suga, T. Room temperature wafer bonding of glass using aluminum oxide intermediate layer. *Adv. Mater. Interfaces* **8**, 2001741 (2021).
33. Takagi, H., Maeda, R., Chung, T. R., Hosoda, N. & Suga, T. Effect of surface roughness on room-temperature wafer bonding by Ar beam surface activation. *Jpn. J. Appl. Phys.* **37**, 4197 (1998).
34. Maszara, W. P., Goetz, G., Caviglia, A. & McKitterick, J. B. Bonding of silicon wafers for silicon-on-insulator. *J. Appl. Phys.* **64**, 4943 (1988).

Acknowledgements

Part of this work was financially supported by Kakenhi Grants-in-Aid (JP20H02207, JP21K18729) from the Japan Society for the Promotion of Science (JSPS).

Author contributions

R.T. conceived of the experiments. R.T., S.M., and K.W. conducted experiments. All authors analyzed the results and reviewed the manuscript.

Competing interests
The authors declare no competing interests.

Additional information
Correspondence and requests for materials should be addressed to R.T.

Reprints and permissions information is available at www.nature.com/reprints.

Publisher's note Springer Nature remains neutral with regard to jurisdictional claims in published maps and institutional affiliations.

Open Access This article is licensed under a Creative Commons Attribution 4.0 International License, which permits use, sharing, adaptation, distribution and reproduction in any medium or format, as long as you give appropriate credit to the original author(s) and the source, provide a link to the Creative Commons licence, and indicate if changes were made. The images or other third party material in this article are included in the article's Creative Commons licence, unless indicated otherwise in a credit line to the material. If material is not included in the article's Creative Commons licence and your intended use is not permitted by statutory regulation or exceeds the permitted use, you will need to obtain permission directly from the copyright holder. To view a copy of this licence, visit http://creativecommons.org/licenses/by/4.0/.

© The Author(s) 2023